

1 **Single-cell sequencing reveals a clonal expansion of pro-inflammatory**
2 **synovial CD8 T cells expressing tissue homing receptors in psoriatic arthritis**

3 Frank Penkava¹, Martin Del Castillo Velasco-Herrera², Matthew D Young², Nicole Yager¹, Alicia Lledo Lara³,
4 Charlotte Guzzo², Ash Maroof⁴, Lira Mamanova², Suzanne Cole⁴, Mirjana Efremova², Davide Simone¹,
5 Chrysothemis C Brown⁵, Andrew L Croxford⁶, Sarah Teichmann², Paul Bowness^{†1}, Sam Behjati^{†*2,7,8}, M Hussein
6 Al-Mossawi^{†*1}

7

8 ¹Nuffield Department of Orthopaedics Rheumatology and Musculoskeletal Sciences, University of Oxford,
9 Oxford, OX3 7LD, UK.

10 ²Wellcome Sanger Institute, Hinxton, CB10 1SA, UK.

11 ³Wellcome Centre for Human Genetics, University of Oxford, Oxford, OX3 7BN, UK.

12 ⁴UCB Pharma, 216 Bath road, Slough, SL1 3WE, UK.

13 ⁵Infection, Inflammation and Rheumatology Section, UCL Great Ormond Street Institute of Child Health,
14 London, WC1N 1EH, UK.

15 ⁶Idorsia Pharmaceuticals Ltd, Drug Discovery Immunology, Hegenhaimermattweg 91, 4123 Allschwill,
16 Switzerland.

17 ⁷Cambridge University Hospitals NHS Foundation Trust, Cambridge, CB2 0QQ, UK.

18 ⁸Department of Paediatrics, University of Cambridge, Cambridge, CB2 0SP, UK

19

20 [†]These authors jointly supervised the work

21 * Co-corresponding authors

22

23

24 **Abstract**

25 **Psoriatic arthritis (PsA) is a debilitating immune-mediated inflammatory arthritis of unknown pathogenesis**
26 **commonly affecting patients with skin psoriasis. We used three complementary single cell approaches to**
27 **study leukocytes from PsA joints. Mass cytometry (CyTOF) demonstrated marked (>3 fold) expansion of**
28 **memory CD8 T cells in the joints compared to matched blood. Further exploration of the memory CD8**
29 **compartment using both droplet and plate based single cell RNA sequencing of paired alpha and beta chain**
30 **T cell receptor sequences identified pronounced CD8 T cell clonal expansions within the joints, strongly**
31 **suggesting antigen driven expansion. These clonotypes exhibited distinct gene expression profiles including**
32 **cycling, activation, tissue homing and tissue residency markers. Pseudotime analysis of these clonal CD8**
33 **populations identified trajectories in which tissue residency can represent an intermediate developmental**
34 **state giving rise to activated, cycling and exhausted CD8 populations. Comparing T-cell clonality across**
35 **patients further revealed specificity convergence of clones against a putative common antigen. We identify**
36 **chemokine receptor *CXCR3* as upregulated in expanded synovial clones, and elevation of two *CXCR3* ligands,**
37 ***CXCL9* and *CXCL10*, in PsA synovial fluid.**

38
39

40 Up to one third of patients suffering from psoriasis develop the debilitating immune-mediated inflammatory
41 joint disease, psoriatic arthritis (PsA)¹. The pathogenesis of PsA is complex, involving multiple inflammatory
42 pathways². Genome-wide association studies of both psoriasis and PsA support a pathogenic role for CD8 T cells,
43 showing significant associations with MHC class I and other T cell genes³. A subgroup of patients with PsA
44 develop a distinct pattern of arthritis, termed large-joint oligo PsA, which affects large joints including the
45 knees⁴. These patients often require therapeutic aspiration which provides an opportunity to examine the
46 synovial exudate in PsA. Here, we study the cellular landscape of PsA blood and synovial fluid at single cell
47 resolution (**Figure 1A**), combining mass cytometry with droplet-encapsulated single cell mRNA sequencing
48 (Chromium 10x) and validation by full length transcript (Smart-seq 2) single cell mRNA sequencing (**Figure 1B**).

49 We first used mass cytometry (CyTOF) to quantify leucocyte populations from matched synovial fluid and blood
50 obtained from 10 patients presenting with large-joint oligo psoriatic arthritis for arthrocentesis (**Figure 1C-D**).
51 Blood and synovial samples were fixed within 30 minutes of collection, stained with a 38-marker panel
52 (**Supplementary Table 1**) and then acquired on a CyTOF Helios instrument. After pre-processing, we used t-

53 stochastic neighbour embedding (tSNE) to derive cell clusters (**Figure 1C**), which were annotated by FlowSOM⁵
54 (**Supplementary Figure 1**). These analyses identified significant expansions in all patients of synovial memory
55 CD8 (p=0.0059, paired t-test) and CD4 (p=0.025, paired t-test) T cells (**Figure 1D-E**) compared to blood. Other
56 populations expanded in synovial fluid were plasmacytoid (p = 0.032, paired t-test) and conventional dendritic
57 cells (p = 0.013, paired t-test) indicating increased capacity for antigen presentation. B cells and basophils were
58 depleted (p = 0.0059 for both, paired t-test), and monocytes, gamma-delta T, mucosal invariant T (MAIT)⁶ and
59 NK cells were unchanged (**Figure 1D**). 3' droplet-encapsulated single cell mRNA sequencing of PBMC and SFMC
60 from three PsA patients, carried out in parallel, confirmed the presence of these cell types and did not identify
61 any additional cellular populations (**Supplementary Figure 1**).

62 To further investigate the significantly expanded memory CD4 and CD8 T cell populations (and supported by the
63 genetic association of PsA with polymorphisms in T cell-related genes⁷), we analyzed transcription and VDJ
64 clonality of matched synovial fluid and blood at single cell resolution. For three patients, we used droplet
65 encapsulated single cell 5' mRNA sequencing (Chromium 10x), with Smart-seq2 validation in four patients
66 (applying both 10x and Smart-seq 2 technology in parallel on the same sorted cells for one donor). For both
67 approaches, synovial fluid and blood were processed in parallel directly *ex vivo* within four hours, with single
68 cell solutions enriched for CD4 and CD8 T cells by flow cytometry activated cell sorting (**Supplementary Figure**
69 **2**). After applying stringent quality control criteria (**Methods**), we studied 39,252 single cell transcriptomes of
70 equal patient and tissue origin using 10x (**Supplementary table 1**), which were integrated using the Seurat 3
71 pipeline to derive cell clusters (**Supplementary Figure 2**). We found 16 clusters of memory CD4 and CD8 T cells
72 in synovial fluid and blood (**Figure 1F**), annotated with key marker genes in **Figure 1G** (**Supplementary Table 1**,
73 **Supplementary Figure 2**). Of note one cluster (cluster 15) derived from all three patients and predominantly
74 composed of synovial CD8 T cells, was distinguished by high expression of the proliferation marker *MKI67*,
75 indicating active proliferation of CD8 T cells within inflamed joints.

76 We next looked for evidence of clonal expansion of CD4 and CD8 T cells in the blood and synovial fluid of each
77 of the three donors using the 10x data set (**Figure 2A-C**). For every individual we observed between 7 and 20
78 CD8 clones (and 1-4 CD4 clones) significantly enriched in the synovial fluid (see **Methods**, **Figure 2C**,
79 **Supplementary Table 2**). For patient PSA1607, parallel Smart-seq 2 data showed the same maximally enriched
80 clone with the same magnitude of clonal expansion (**Figure 2K**, **Supplementary Table 2**). To determine whether

81 clonal expansion of CD8 or CD4 T cells may be driven by common antigen(s), we used the Grouping of
82 Lymphocyte Interactions by Paratope Hotspots (GLIPH)⁸ algorithm to assess TCR complementarity-determining
83 region 3 (CDR3) similarity and putative shared specificity across the three patients in the 10x experiment. GLIPH
84 analysis of 40915 synovial cells with 19582 unique CDR3 beta chain amino acid sequences revealed 143 TCR
85 convergence groups (CRG) with shared specificity between the three patients (**Supplementary table 4**). One
86 CRG in particular, contained a high number of cells belonging to synovial enriched CD8 clones, including the
87 most enriched clones from 2 patients ($p = 4.2E-27$ and $2.1E-112$ for patients PSA1505 and PSA1607 respectively),
88 and bearing a GLIPH identified enriched CDR3 "NQNT" motif (observed versus expected foldchange 10.869, $p =$
89 0.001) relative to the expected frequency in an unselected naive reference TCR set⁸.

90 To validate these specificity groups we studied a further 1441 synovial CD4 and CD8 T cells with 1236 unique
91 beta chain CDR3 amino acid sequences from three independent patients in the Smart-seq 2 data set. GLIPH
92 analysis incorporating these sequences with the original 10x TCR sequences obtained from 40915 cells identified
93 5 TCR specificity groups common to all 6 patients. One of these 5 groups (CRG-1) was again assigned the "NQNT"
94 motif and incorporated the same clones as the synovial-enriched CRG identified by droplet-encapsulated data
95 alone (**Figure 2D-E and Supplementary Table 4**). These findings provide evidence that CD8 lymphocyte
96 expansion in psoriatic arthritis is driven by common antigens across patients, arguing against cytokine or
97 superantigen-driven expansion.

98 CRG-1 contributed the greatest number of expanded clones to the observed CD8 T cell expansions in synovial
99 fluid and displayed high usage of the TCR genes *TRBV28* and *TRBJ1-1* (**Figure 2F**). Of note, cells from CRG-1 were
100 predominantly assigned to synovial cell clusters 4 and 10 (**Figure 2G-H**). Transcripts defining cluster 4 (**Figure 2I**)
101 included granzyme (*GZMA*, *GZMB*, *GZMH* and *GZMK*), *CCL4*, *CCL5*, *CD74* and MHC-II, indicating an activated
102 phenotype. Cluster 10 defining transcripts (**Figure 2J**) included *KLRC1* (NKG2A), the tissue-residency marker
103 *ZNF683*⁹, the skin/gut homing marker *ITGA1*(CD49a)¹⁰ and granulysin (*GNLY*). These two distinct CD8 clusters
104 were also reported in a recent single-cell study of synovial tissue CD8 cells in rheumatoid arthritis¹¹. When
105 integrating 10x and smart-seq 2 gene expression data from the same patient, we observed cells from clones
106 maximally enriched in synovial fluid from each technology within the same cluster, validating our approach
107 (**Figure 2K, Supplementary Figure 3, Supplementary Tables 1 and 2**). The cells within CRG-1 showed a similar
108 gene expression profile compared to their non-CRG-1 neighbours within the same cluster (**Supplementary**

109 **Figure 4**). Cells from both clusters 4 and 10 showed an overlapping gene signature with previously described
110 tissue-resident epidermal skin CD49a⁺ CD8 T cells "poised for cytotoxic function" (**Supplementary Figure 4**),
111 which were also shown to be enriched for specific TCR V gene usage including *TRBV28*¹². Pseudotime analysis of
112 all cells identified within CRG-1 showed two trajectories of differentiation for CD8 cells. Trajectory one (**Figure**
113 **2L**) begins with a central memory phenotype which then transitions from tissue residency to activated
114 phenotypes before entering active cell cycle. This trajectory accounts for the clonal expansion we observe in the
115 synovial compartment. Trajectory two (**Figure 2M**) also arises from the central memory phenotype and passes
116 from tissue to activated states but then diverges to an exhausted phenotype. When we follow the single most
117 expanded clone in the synovial compartment of one patient, we observe that this same clone contains cells that
118 have predominantly central memory, tissue, transitional, activated and cycling phenotypes (**Figure 2K**).
119 Pseudotime analysis of this single expanded clone shows the same shared central memory to transitional CD8
120 trajectory with either activated or cycling end states (**Figure 2N and Supplementary Figure 3**). We propose that
121 the CD8 tissue resident phenotype is derived from the central memory compartment and following tissue
122 activation, can follow trajectories giving rise to activated/cycling and exhausted synovial CD8 populations. This
123 bifurcation in T cell fate has previously been reported in response to infectious challenge.¹³

124 Comparison of blood and synovial fluid TCR clonotypes showed that some clonotypes were present at both sites,
125 highlighting inhibition of CD8 T cell trafficking as a specific therapeutic opportunity. To look for mRNAs that
126 might mediate trafficking, we compared transcriptomes of synovial and blood T cells from clones significantly
127 enriched in synovial fluid (n= 1,750 cells) and blood (n= 828 cells) respectively. Subsetting and re-clustering of
128 these 2,578 cells yielded 7 clusters (**Figure 3A-C, Supplementary Table 3**) mapping back to the original clustering
129 analysis (**Figure 1F-G**). Genes encoding chemokine receptors *CCR1*, *CCR5*, *CXCR3* and *CXCR6* were highly
130 expressed in synovial-enriched T cell clones (**Figure 3C**), with particularly elevated *CXCR3* gene expression
131 (adjusted p = 7.6E-29 for activated CD8 cluster, adjusted p = 3.4E-6 for exhausted CD8 cluster, Wilcoxon rank
132 sum test). The over-expression of *CXCR3* in synovial T cells was striking when mapped back to the whole 10x 5'
133 data set (**Figure 3D-E**). To functionally validate this finding, we measured protein levels of IP10 (CXCL10) and
134 CXCL9 (ligands for CXCR3), together with MIP1 α (CCL3) and MIP1 β (CCL4) (ligands for CCR1 and CCR5
135 respectively), in the plasma and synovial fluid of patients with psoriatic arthritis (**Figure 3F**). Both CXCR3 ligands
136 were highly enriched in the synovial fluid compared to blood (p = 0.0004 for CXCL10, p = 0.007 for CXCL9, paired

137 t-test). CXCR3 is known to be expressed on activated Th1 and CD8 T cells and plays a key role in chemotaxis
138 during inflammation^{14,15}. Interestingly, CXCR3-expressing T cells have previously been shown to be depleted in
139 peripheral blood of patients with psoriasis, which had been speculated to be due to recruitment of these cells
140 into skin lesions¹⁶. Our findings raise the possibility that CXCR3+ CD8 T cells play a central role in executing
141 localised inflammation in PsA and thus represent an attractive therapeutic target. Further analysis revealed that
142 cells belonging to CRG-1 and cells from related clusters 4, 10 and 15 had selectively higher *CX3CR1* gene
143 expression in blood (**Supplementary Figure 4**), potentially providing additional means to identify and target
144 convergence group related CD8 T cells in blood.

145 In this study we have defined and characterized clonal expansions of CD8 T cells in the joints of patients with
146 PsA, previously suggested using bulk sequencing techniques¹⁷, using three complementary single-cell
147 approaches. The presence of expanded clones expressing markers of activation, tissue residency and/or tissue
148 homing with evidence of shared TCR recognition across patients provides the strongest evidence yet that
149 psoriatic arthritis is an MHC-I antigen driven disease. Pseudotime analysis of cells with convergent antigen
150 specificity (CRG-1) as well as individually expanded clones provides evidence of differentiation from central
151 memory to tissue phenotypes and insight into how this tissue-resident niche is populated in humans¹⁸. With
152 application of novel approaches to identify antigens using MHC/peptide phage-display libraries¹⁹ or to
153 potentially predict antigens directly from TCR sequences, these data will in future allow us to define the nature
154 of antigens that drive psoriatic arthritis.

155 **Methods Summary**

156

157 **Study subjects**

158 Blood and synovial fluid samples were collected with full informed patient consent from PsA patients
159 undergoing intra-articular aspiration at Oxford University Hospitals. The study was performed in accordance
160 with protocols approved by the Oxford Research Ethics committee (Ethics reference number
161 06/Q1606/139).

162

163 **CyTOF staining and analysis**

164 Whole blood or synovial fluid were fixed with high-purity paraformaldehyde within 30 minutes of sample
165 collection. Fixed blood was lysed with Permeabilization Buffer (eBioscience). Cells were stained in Maxpar
166 staining buffer (Fluidigm) with antibodies listed in Supplementary Table 1. Samples were run on a Helios
167 system alongside normalization beads (Fluidigm). As samples were run fresh, each paired sample was

168 analysed separately using a custom R workflow previously described¹⁸, with cell populations clustered using
169 the FlowSOM algorithm⁵.

170

171 **Cell isolation for flow cytometry cell sorting**

172 SFMCs and PBMCs were freshly isolated within 30 minutes of sample collection by density-gradient
173 centrifugation using Histopaque (Sigma). Cells were stained immediately and FACS sorted for droplet based
174 single cell RNA sequencing. Single cell suspensions of freshly isolated paired SFMC and PBMC samples from
175 3 patients were stained by a panel of fluorescently conjugated antibodies in staining buffer (RNase-free PBS,
176 2mM EDTA). The following antibodies were used: CD3-FITC (SK7), CD4-APC (RPA-T4), CD8a-PE (RPA-T8),
177 CD45RA-BV421 (HI100) (all BioLegend), together with eFluor780 viability dye (eBioscience). Memory-
178 enriched (CD45RA negative) CD3+CD4+CD8- and CD3+CD8+CD4- cells were sorted in a 1:1 ratio from both
179 blood and synovial fluid of patients.

180

181 **Droplet based single cell RNA sequencing**

182 Sorted memory-enriched CD4 and CD8 T cell suspensions from peripheral blood and synovial fluid were
183 prepared. Cells were counted and loaded into the Chromium controller (10x-Genomics) chip following the
184 standard protocol for the Chromium single cell 5' Kit (10x Genomics). Total time taken from sample retrieval
185 to sample on the chip was 4 hours. A cell concentration was used to obtain an expected number of captured
186 cells between 5000-10000 cells. All subsequent steps were done based on the standard manufacturer's
187 protocol. Libraries were pooled and sequenced across multiple Illumina HiSeq 4000 lanes to obtain a read
188 depth of approximately 30,000 reads per cell for gene expression libraries and 8500 reads per cell for V(D)J
189 enriched T cell libraries.

190

191 **Plate based single cell RNA-sequencing**

192 Freshly sorted CD45RA negative CD3+CD4+ and CD3+CD8+ single cells from four patients were individually
193 flow sorted into 96-well full-skirted plates (Eppendorf) containing 10 μ L of a 2% Dithiothreitol (DTT, 2M
194 Sigma-Aldrich), RTL lysis buffer (Qiagen) solution. Cell lysates were sealed, mixed and spun down before
195 storing at -80 °C. Paired-end multiplexed sequencing libraries were prepared following the Smart-seq2 (SS2)
196 protocol²¹ using the Nextera XT DNA library prep kit (Illumina). A pool of barcoded libraries from four
197 different plates were sequenced across two lanes on the Illumina HiSeq 2500.

198

199 **Droplet based single cell RNA-seq data mapping and pre-processing**

200 The raw single-cell sequencing data was mapped and quantified using the 10x Genomics Inc. software
201 package Cell Ranger (v2.1) against the GRCh38 reference provided by 10x with that release. Using the table
202 of unique molecular identifiers produced by Cell Ranger, we identified droplets that contained cells using
203 the call of functional droplets generated by Cell Ranger.

204

205 **Quality control of droplet based single cell expression data**

206 After cell containing droplets were identified, gene expression matrices were first filtered to remove cells
207 with > 10% mitochondrial genes, < 500 or > 3500 genes, and > 25000 UMI. Cells were further filtered to
208 include only cells with corresponding CDR3 TCR data and to exclude potential multiplets, defined as cells
209 with greater than 1 beta chain or 2 alpha chains or cells having both CD4 and CD8 gene expression (given
210 the sorting strategy used).

211

212 **Quality control of SS2 based single cell expression data**

213 Cells with more than 5 median absolute deviations (MAD) 8.35% of their mRNA originating from
214 mitochondrial genes; a total number of reads <500,000 or > 5000000; a total number of counts >3 median
215 absolute deviations (MAD); or with number of genes <1000 or > 6000, were filtered out prior to downstream
216 analysis. Where matching TCR data for a cell was available, any cells with greater than 1 beta chain or 2
217 alpha chains were additionally filtered.

218

219 **Droplet based integrated gene expression analysis of peripheral blood and synovial fluid from 3 patients**

220 Cellranger output included 6 expression matrices (3 patients, each with paired blood and synovial fluid
221 samples) and downstream analyses of these matrices was carried out using R (3.6.0) and the Seurat package
222 (v 3.0.2, satijalab.org/seurat). After quality control filtering, data were subsampled to include an equal
223 number of cells from blood and synovial fluid from all patients (6542 cells per sample, totaling 39252 cells).
224 All 6 data sets were then individually normalised and variable genes discovered using the SCTransform
225 function with default parameters, providing total number of UMIs and mitochondrial fraction as factors to
226 regress out. The FindIntegrationAnchors function command was subsequently run with default parameters
227 (dims = 1:30) to discover integration anchors across all samples. Any TCR genes were excluded from anchor
228 features discovered prior to downstream analysis, and the IntegrateData function was run on this reduced
229 anchorset with default additional arguments. ScaleData and RunPCA were then performed on the integrated
230 assay to compute 30 principal components (PC). Uniform Manifold Approximation and Projection (UMAP)
231 dimensionality reduction was carried out and Shared Nearest Neighbor (SNN) graph constructed using
232 dimensions 1:30 as input features and default PCA reduction. Clustering was performed on the Integrated
233 assay at a resolution of 0.7 with otherwise default parameters which yielded a total of 16 clusters, each
234 composed of cells originating from both blood and synovial fluid from all 3 patients and classified by
235 differentially expressed genes. (**Supplementary Figure 2**).

236

237 To compare synovial (1750) and blood (828) cells from synovial and blood enriched clones respectively, all
238 significantly enriched clones from both tissues were isolated from the previously filtered integrated data set
239 using the SubsetData function. The integrated assay of this subset was scaled using the ScaleData function
240 before running principal component analysis. Dimensionality reduction was calculated with UMAP using the
241 first 20 principal components and clustering set at a resolution of 0.4 to reflect the smaller cell numbers
242 relative to the parent data set. This yielded 7 clusters.

243

244 **Droplet and SS2 based integrated gene expression analysis of PSA1607 peripheral blood and synovial fluid**

245 For validation of sequencing data across platforms, quality control filtered 10x expression matrices from 1
246 patient (PSA1607) were subsampled to include an equal number of cells from blood and synovial fluid (
247 11192 cells from each, totaling 22384 cells). Quality control filtered SS2 data matrices from this same patient
248 were similarly subsampled to include 433 cells from both blood and synovial fluid. The same steps outlined
249 above for integration of droplet based only data sets from 3 patients were used to integrate these 4 data
250 sets (blood and synovial from both 10x and SS2 platforms) for patient PSA1607. Apart from additionally
251 regressing out platform when scaling data, the same optional arguments specifying 30 principal components
252 and a cluster resolution of 0.7 were used. This yielded 13 clusters which were again classified by differentially
253 expressed genes, bearing gene expression signatures that overlapped with clusters identified in the 10x only
254 integration of 3 patients (**Supplementary figure 3, Supplementary Table 1**).

255

256

257

258 **TCR mapping**

259 Chromium 10x V(D)J single-cell sequencing data was mapped and quantified using the software package
260 Cell Ranger (v2.1) against the GRCh38 reference provided by 10x Genomics with that release. The generated
261 consensus annotations files for each patient and sample type (blood or synovial fluid) were then used to
262 construct clonality tables and input files for further downstream analysis. Full-length, paired T cell receptor
263 (TCR) nucleotide sequences from SS2 data were constructed using the TraCeR program²², and further
264 mapped to V, D and J genes as well as CDR3 nucleotide and amino acid sequences using the online IMGT-
265 HighVQuest tool²³. The software package GLIPH v 1.0 was used to construct and assess specificity groups⁸.
266 As the GLIPH algorithm only makes use of single CDR3 beta chain amino acid sequences to associate clones
267 of common specificity, multiple beta chain sequences within the same partition were treated as multipliers
268 and provided as separate individual sequences to GLIPH (annotated with a "v" suffix). Partitions containing
269 only alpha chain sequences were excluded from GLIPH input. The VDJtools 1.1.8²⁴ software package was
270 used to construct circle plots illustrating V(D)J gene usage.

271

272 To assess clonal enrichment, the proportion of cells having the same clone was compared between sample
273 types for each clone using a Fisher's exact test with Benjamini & Hochberg (1995) correction for multiple
274 comparisons (R Stats Package). A cell's clonotype was defined as the combined alpha and beta chain CDR3
275 nucleotide sequences for that cell. As it was not possible to deduce beta and alpha chain pairing for
276 partitions with multiple beta chains, these partitions were treated as a single clone.

277

278 **Plate based single cell RNA-sequencing expression quantification**

279 To assess the expression from the SS2 data, raw reads were pseudo-mapped and counted using kallisto
280 v0.43.1²³ based on the annotation made by ENSEMBL(v90) of the human reference genome (GRCh38). To
281 obtain per gene counts, all of the transcript counts were summarised using scater v1.6.3²⁶.

282

283 **Chemokine protein quantification**

284 Paired plasma and synovial fluid supernatant was collected from patients undergoing knee aspiration
285 procedures and frozen at -80°C within one hour of sample collections. Samples were thawed and chemokine
286 protein quantification was performed using a LEGENDplex™ Human Proinflammatory Chemokine Panel (13-
287 plex) immunoassay (Cat# 740003) according to the manufacturer's instructions. Samples were acquired on
288 two different dates, with similar results obtained. The data was acquired on a Novocyte instrument and
289 analyzed using the LEGENDplex™ Data Analysis Software provided by BioLegend

290

291 **Statistical Analyses**

292 Statistical tests were performed as indicated in the figure legends.

293

294 **Data availability**

295 The raw sequencing data generated for the present study has been deposited in the European Genome-
296 phenome Archive.

297 References:

- 298 1. Ibrahim, G., Waxman, R. & Helliwell, P. S. The prevalence of psoriatic arthritis in people with psoriasis.
299 *Arthritis Care Amp Res.* **61**, 1373–1378 (2009).
- 300 2. Veale, D. J. & Fearon, U. The pathogenesis of psoriatic arthritis. *The Lancet* **391**, 2273–2284 (2018).
- 301 3. Stuart, P. E. *et al.* Genome-wide Association Analysis of Psoriatic Arthritis and Cutaneous Psoriasis Reveals
302 Differences in Their Genetic Architecture. *Am. J. Hum. Genet.* **97**, 816–836 (2015).
- 303 4. Moll, J. M. H. & Wright, V. Psoriatic arthritis. *Semin. Arthritis Rheum.* **3**, 55–78 (1973).
- 304 5. Van Gassen, S. *et al.* FlowSOM: Using self-organizing maps for visualization and interpretation of
305 cytometry data. *Cytom. Part J. Int. Soc. Anal. Cytol.* **87**, 636–645 (2015).
- 306 6. Walker, L. J. *et al.* Human MAIT and CD8 α cells develop from a pool of type-17 precommitted CD8+ T
307 cells. *Blood* **119**, 422–433 (2012).
- 308 7. Ellinghaus, E. *et al.* Genome-wide meta-analysis of Psoriatic Arthritis Identifies Susceptibility Locus at REL.
309 *J. Invest. Dermatol.* **132**, 1133–1140 (2012).
- 310 8. Glanville, J. *et al.* Identifying specificity groups in the T cell receptor repertoire. *Nature* **547**, 94–98 (2017).
- 311 9. Mackay, L. K. *et al.* Hobit and Blimp1 instruct a universal transcriptional program of tissue residency in
312 lymphocytes. *Science* **352**, 459–463 (2016).
- 313 10. Kumar, B. V. *et al.* Human tissue-resident memory T cells are defined by core transcriptional and
314 functional signatures in lymphoid and mucosal sites. *Cell Rep.* **20**, 2921–2934 (2017).
- 315 11. Zhang, F. *et al.* Defining inflammatory cell states in rheumatoid arthritis joint synovial tissues by
316 integrating single-cell transcriptomics and mass cytometry. *Nat. Immunol.* **20**, 928 (2019).
- 317 12. Cheuk, S. *et al.* CD49a Expression Defines Tissue-Resident CD8+ T Cells Poised for Cytotoxic Function in
318 Human Skin. *Immunity* **46**, 287–300 (2017).
- 319 13. Lönnberg, T. *et al.* Single-cell RNA-seq and computational analysis using temporal mixture modeling
320 resolves TH1/TFH fate bifurcation in malaria. *Sci. Immunol.* **2**, eaal2192 (2017).
- 321 14. Smit, M. J. *et al.* CXCR3-mediated chemotaxis of human T cells is regulated by a Gi- and phospholipase C-
322 dependent pathway and not via activation of MEK/p44/p42 MAPK nor Akt/PI-3 kinase. *Blood* **102**, 1959–
323 1965 (2003).

- 324 15. Kurachi, M. *et al.* Chemokine receptor CXCR3 facilitates CD8+ T cell differentiation into short-lived effector
325 cells leading to memory degeneration. *J. Exp. Med.* **208**, 1605–1620 (2011).
- 326 16. Lima, X. T. *et al.* Circulating levels of chemokines in psoriasis. *Autoimmunity* **48**, 57–60 (2015).
- 327 17. Costello, P. J. *et al.* Psoriatic Arthritis Joint Fluids Are Characterized by CD8 and CD4 T Cell Clonal
328 Expansions that Appear Antigen Driven. *J. Immunol.* **166**, 2878–2886 (2001).
- 329 18. Dijkgraaf, F. E. *et al.* Tissue patrol by resident memory CD8 + T cells in human skin. *Nat. Immunol.* **20**, 756
330 (2019).
- 331 19. Birnbaum, M. E. *et al.* Deconstructing the peptide-MHC specificity of T cell recognition. *Cell* **157**, 1073–
332 1087 (2014).
- 333 20. Nowicka, M. *et al.* CyTOF workflow: differential discovery in high-throughput high-dimensional cytometry
334 datasets. *F1000Research* **6**, 748 (2017).
- 335 21. Picelli, S. *et al.* Full-length RNA-seq from single cells using Smart-seq2. *Nat. Protoc.* (2014).
336 doi:10.1038/nprot.2014.006
- 337 22. Stubbington, M. J. T. *et al.* T cell fate and clonality inference from single-cell transcriptomes. *Nat. Methods*
338 **13**, 329–332 (2016).
- 339 23. Aouinti, S., Malouche, D., Giudicelli, V., Kossida, S. & Lefranc, M.-P. IMGT/HighV-QUEST Statistical
340 Significance of IMGT Clonotype (AA) Diversity per Gene for Standardized Comparisons of Next Generation
341 Sequencing Immunoprofiles of Immunoglobulins and T Cell Receptors. *PLOS ONE* **10**, e0142353 (2015).
- 342 24. Shugay, M. *et al.* VDJtools: Unifying Post-analysis of T Cell Receptor Repertoires. *PLOS Comput. Biol.* **11**,
343 e1004503 (2015).
- 344 25. Bray, N. L., Pimentel, H., Melsted, P. & Pachter, L. Near-optimal probabilistic RNA-seq quantification. *Nat.*
345 *Biotechnol.* **34**, 525–527 (2016).
- 346 26. McCarthy, D. J., Campbell, K. R., Lun, A. T. L. & Wills, Q. F. Scater: pre-processing, quality control,
347 normalization and visualization of single-cell RNA-seq data in R. *Bioinformatics* **33**, btw777 (2017).
- 348

349 **Acknowledgements**

350 We thank Jon Webber and Catherine Simpson for assistance with cell sorting. We are grateful to Muzlifah Haniffa
351 for critical review of the manuscript. The research was funded by The Kennedy Trust Studentship (FP), The
352 Academy of Medical Sciences Grant to HA (SGL018\1006) and Personal fellowship support HA (Oxford-UCB Prize
353 fellowship) SB (Wellcome; St Baldrick's Foundation), CB (Wellcome). PB and HA are also funded by the National
354 Institute for Health Research (NIHR) Oxford Biomedical Research Centre (BRC). The views expressed are those
355 of the author(s) and not necessarily those of the NHS, the NIHR or the Department of Health.

356

357 **Author Contributions.**

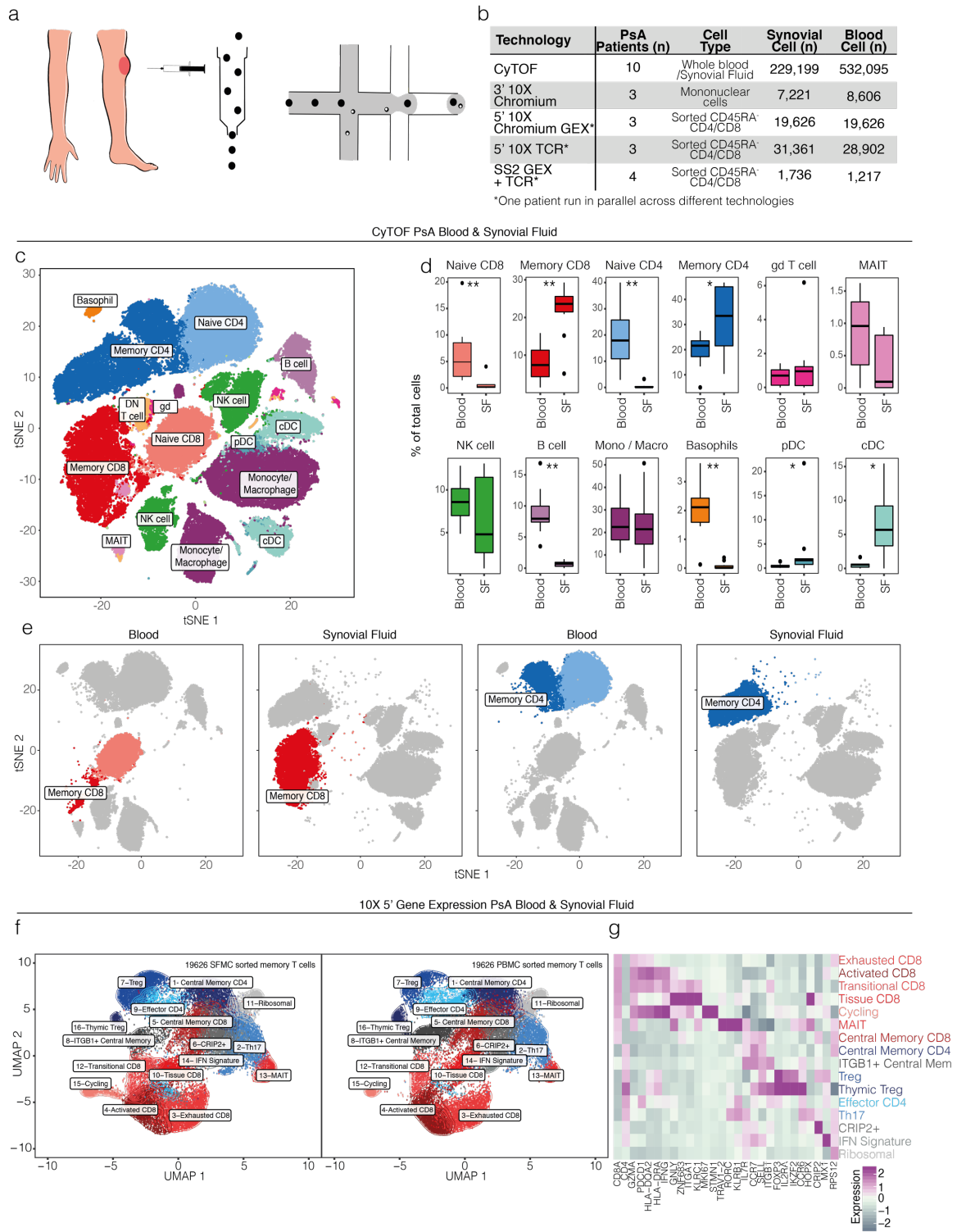
358 HA-M and SB conceived and designed the experiments; FP and HA-M performed the 10x experiments,
359 designed and performed computational analysis aided by MDCVH, MDY, LM, ME and DS ; MDCVH
360 performed the SMART-seq2 experiments assisted by CG and LM ; NY performed the CyTOF experiments
361 assisted by ALL, SC and AM ; NY, ALL and SC performed flow cytometry and assisted with cell-sorting; ALC
362 performed protein quantification assays ; ST and CB contributed to discussions; HA-M, SB and PB wrote the
363 manuscript, PB, SB and HA-M co-directed this study.

364

365 **Author Information.**

366 The authors declare no conflict of interest. Correspondence and requests for materials should be
367 addressed to sb31@sanger.ac.uk and hussain.al-mossawi@ndorms.ox.ac.uk.

368 Figure 1



370 **Figure 1. Landscape of synovial leukocyte populations in Psoriatic Arthritis**

371 a. Overview of experimental design.

372 b. Cell numbers used in each of the experimental techniques.

373 c. Representative map of CyTOF clusters derived from PsA matched peripheral blood and synovial fluid cells
374 using t-SNE.

375 d. Cluster frequencies across blood and synovial fluid (SF), n= 10, paired t-test. (* = $p<0.05$, ** = $p<0.01$, *** =
376 $p<0.001$).

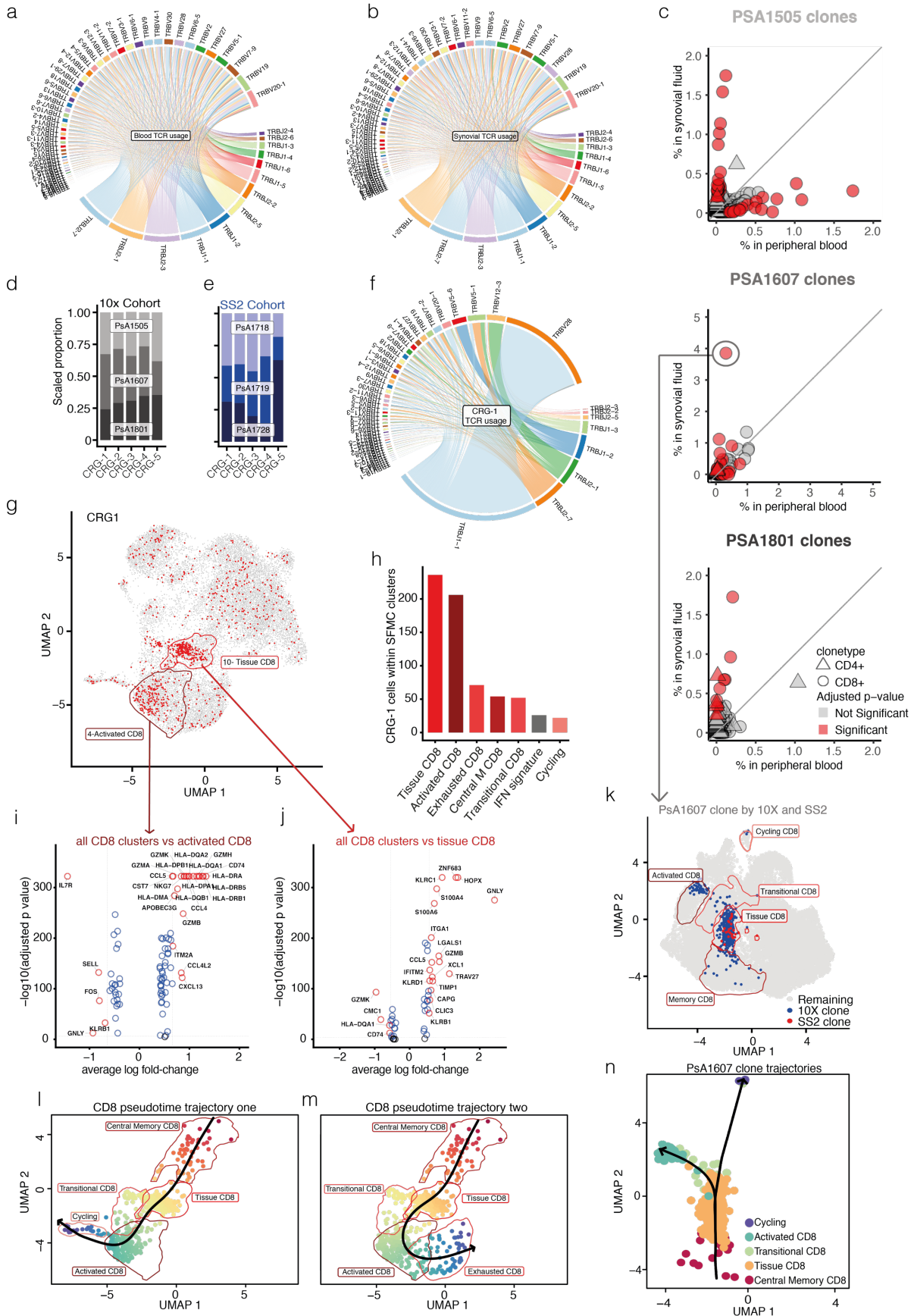
377 e. Representative map of CyTOF clusters divided according to tissue of origin and highlighting memory CD8
378 and memory CD4 T cells.

379 f. UMAP of sorted synovial (left) and blood(right) memory CD4 and CD8 T cells from 3 donors after integration.
380 Clusters coloured red are comprised of CD8 cells, clusters coloured blue are CD4 cells. Clusters in grey contain
381 mixed CD4 and CD8 populations.

382 g. Heatmap showing memory CD4 and CD8 immune subset signatures. The relative expression of marker genes
383 (columns) across cell clusters (rows) is shown.

384

385 **Figure 2**



387 **Figure 2. Synovial CD8 clonal expansion in Psoriatic Arthritis**

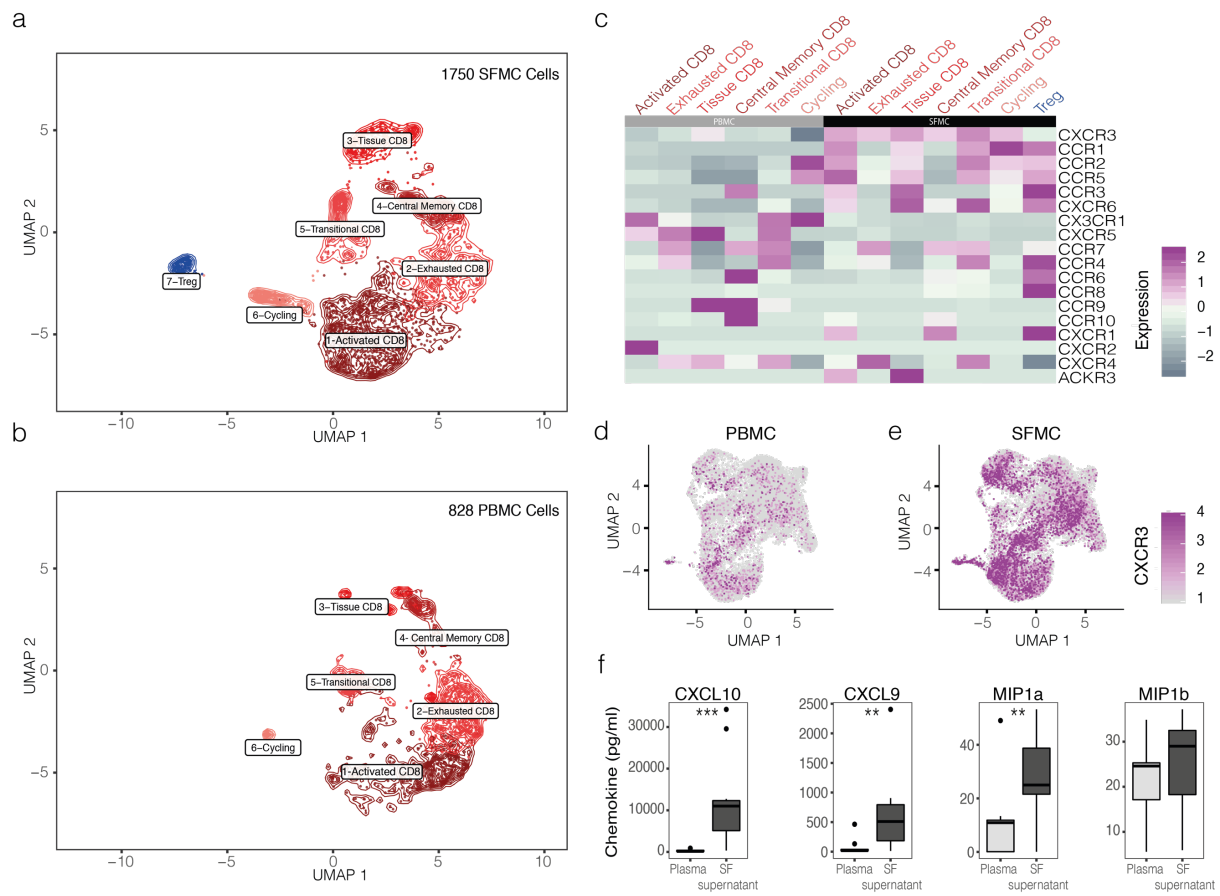
- 388 **a-b.** TCR beta chain V and J gene usage in PsA blood and synovial fluid generated from 10x 5' data.
- 389 **c.** Clonal expansion across blood and synovial fluid in three PsA patients based on 10x 5' data. Circles represent
- 390 CD8 clonotypes, triangles represent CD4 clonotypes. Data points coloured red show significantly expanded
- 391 clonotypes. Fisher's exact test, Benjamini-Hochberg correction.
- 392 **d.** Patient distribution of top 5 GLIPH convergence groups (CRG) in 5' 10x data set.
- 393 **e.** Patient distribution of top 5 GLIPH CRG in Smart-seq 2 (SS2) data set.
- 394 **f.** TCR beta chain V and J gene usage in GLIPH CRG-1.
- 395 **g.** Cells from CRG-1 highlighted on UMAP plot of all SFMC derived T cells from 5' 10x data set.
- 396 **h.** Number of CRG-1 cells within each of the synovial T cell clusters.
- 397 **i.** Volcano plot showing differential gene expression of SF CD8 T cells in cluster 4 (Activated CD8) vs all other SF
- 398 CD8 T cells, statistical significance calculated using Wilcoxon rank sum test. (Supplementary table 1)
- 399 **j.** Volcano plot showing differential gene expression of SF CD8 T cells in cluster 10 (Tissue CD8) vs all other SF
- 400 CD8 T cells, statistical significance calculated using Wilcoxon rank sum test. (Supplementary table 1)
- 401 **k.** UMAP plot of integrated memory T cells from one donor (PSA1607) including cells from 5' 10x and SS2 data
- 402 sets (Supplementary Figure 3). Synovial CD8 T cells from the clone most enriched in synovial fluid for this
- 403 patient is highlighted in blue for the 10x data set and red for the SS2 data set.
- 404 **l.** Pseudotime analysis of CRG-1 CD8 T cells showing first trajectory differentiation pathway from central
- 405 memory phenotype to tissue residency and activated states before entering cell cycle. Cells coloured by
- 406 pseudotime from red to dark blue.
- 407 **m.** Pseudotime analysis of CRG-1 CD8 T cells showing second trajectory differentiation pathway from central
- 408 memory phenotype to tissue residency and activated states before terminating in exhausted phenotype. Cells
- 409 coloured by pseudotime from red to dark blue.
- 410 **n.** Pseudotime analysis of largest synovially enriched clone from donor PSA1607 showing shared central
- 411 memory and tissue trajectory ending in either activated or cycling cell state (with no exhausted end state).
- 412 Cells are coloured by phenotypic cluster to which they belong (Supplementary figure 3).

413

414

415

416 **Figure 3**



417

418 **Figure 3. Clonal T cell trafficking in Psoriatic Arthritis**

419 **a-b.** UMAP of 2578 (1750 synovial, 828 peripheral blood) T cells from clones significantly enriched in PsA

420 synovial fluid and blood respectively, split by tissue of origin. Synovial cells in panel **a**, peripheral blood cells in
421 panel **b**.

422 **c.** Heatmap of significantly expanded blood and synovial T cell clone clusters (columns) split by tissue of origin
423 and showing chemokine receptor expression (rows).

424 **d.** UMAP of whole 5' 10x data set of T cells derived from PBMC with *CXCR3* expression highlighted.

425 **e.** UMAP of whole 5' 10x data set of T cells derived from SFMC with *CXCR3* expression highlighted.

426 **f.** CXCL10, CXCL9, MIP1 α and MIP1 β protein quantification by LegendPlex in paired plasma and synovial fluid
427 supernatant from PsA patients, n= 10, paired t-test (** = p<0.01, *** = p<0.001).

428